9.14 PIV in Reacting Flows

Contributed by:
C. Willert

Application of PIV in reacting flows is associated with a number of additional challenges not found in typical aerodynamic applications. Most importantly the seed material must withstand the high temperatures without evaporat-

Table 9.19. PIV recording parameters for reactive flow in pressurized combustor

Flow geometry	swirling flow with strong out-of-plane component near nozzle
Maximum in-plane velocity	$U_{\max} \approx 70\,\mathrm{m/s}$
Field of view	$70 \times 40\,\mathrm{mm}^2$ $(W \times H)$
Interrogation volume	$1.7 \times 1.7 \times 1.0\,\mathrm{mm}^3$ $(W \times H \times D)$
Dynamic spatial range	DSR $\approx 40:1$
Dynamic velocity range	DVR $\approx 120:1$
Observation distance	$z_0 \approx 500\,\mathrm{mm}$
Recording method	dual frame/single exposure
Ambiguity removal	frame separation (frame-straddling)
Recording medium	full frame interline transfer CCD 1280×1024 pixels (770 illuminated lines)
Recording lens	$f = 55\,\mathrm{mm}$ $f_\# = 8$
Illumination	Freq. doubled Nd:YAG laser $120\,\mathrm{mJ/pulse}$ at $532\,\mathrm{nm}$
Pulse delay	$\Delta t = 4\,\mu\mathrm{s}$
Seeding material	Si_2O_3 and Al_2O_3 ($d_\mathrm{p} \approx 200 - 800\,\mathrm{nm}$)

ing or chemically interacting with the flow under investigation. Metal oxide powders such as silica, alumina or titanium oxide are generally well suited for this purpose due to their high melting point and availability. These powders are best introduced into the flow using fluidized bed seeders as described in section 2.2.2.

Another difficulty arises due to flame luminosity which generally increases with higher pressures and higher fuel-air ratios and is mainly caused due to glowing soot. This flame luminosity can be reduced by placing a narrow-bandwidth interference filter tuned to the wavelength of the PIV laser in front of the sensor or collecting lens. Due to the rather long sensor exposure of the second image frame in modern PIV cameras, this filter may however be insufficient in the suppression of the flame luminosity. Here fast acting electro-mechanical or electro-optical shutters [375, 377] are required. Alternatively a pair of CCDs could be used, each synchronized to one of the two PIV laser pulses [111].

The pressurized single sector combustor, schematically shown in figure 9.75, can be operated at up to 20 bar with air preheating of up to 850 K at mass flow rates of 1.5 kg/s. The nozzle plenum is supplied with preheated primary air downstream of a critical throttle. The primary air is split in a 2:1 ratio and guided into the double swirl nozzle and the inner window cooling slits, respectively. The pressure and mass flow in the chamber is controlled through a sonic orifice at the exit. Jets in cross-flow arrangement at a roughly mid-length position of the 250 mm long combustor provide preheated mixing air and confine the primary zone to a roughly cubic volume.

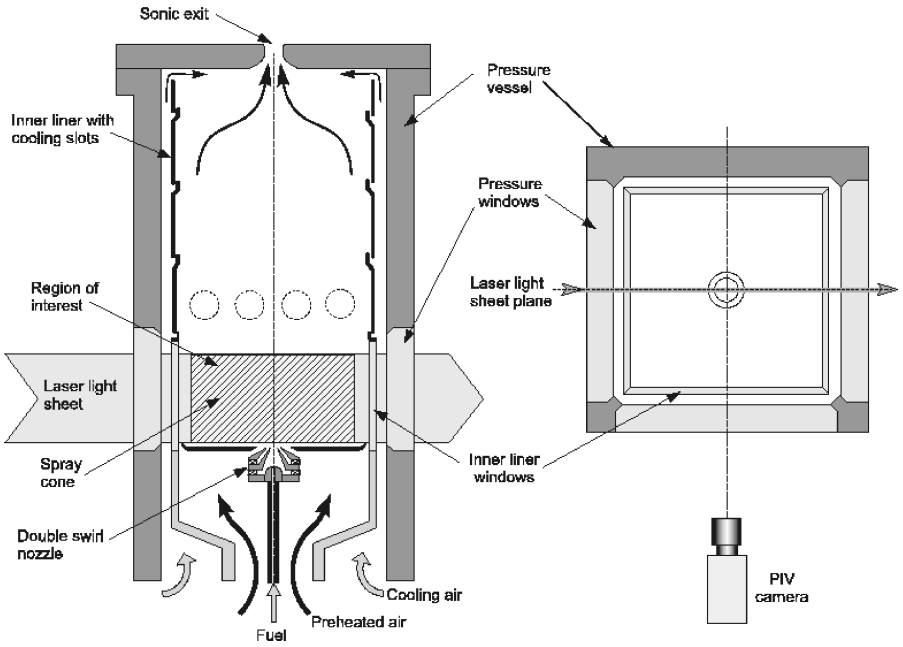

Fig. 9.75. Single sector pressurized combustion facility. Right: cross-sectional axial view.

Optical access is granted from three sides through windows consisting of a thick pressure window and a thin liner window. The gap between the windows is purged with cooling air while the inside of the liner window is film-cooled using a portion of the plenum air. For PIV the light sheet was aligned with the burner axis with the camera arranged in a classical light sheet normal viewing arrangement. By allowing the laser light sheet to pass straight through the combustor the amount of laser flare on imaging windows and walls could be kept at an acceptable level. Seeding consisting of amorphous silicon dioxide particles was introduced to the plenum upstream of the burner through a porous annular tube. As the window film-cooling is supplied directly with seeded air from the plenum, the windows are unfortunately subjected to an accelerated build-up of seeding deposits. Preferably the film-cooling air should have been separated from the main burner air. Fired with kerosene the combustor provided PIV images exhibiting strong Mie scattering off the kerosene spray as well as strong flame luminosity. A corresponding PIV result obtained at lean operating conditions with less kerosene spray is provided in figure 9.76. Image enhancement as shown in figure 9.77 was applied prior to PIV processing and reduced the influence of droplet velocities on the air flow velocity estimates by equalizing the droplet image intensities with the much weaker intensity of the seeding particles [377].

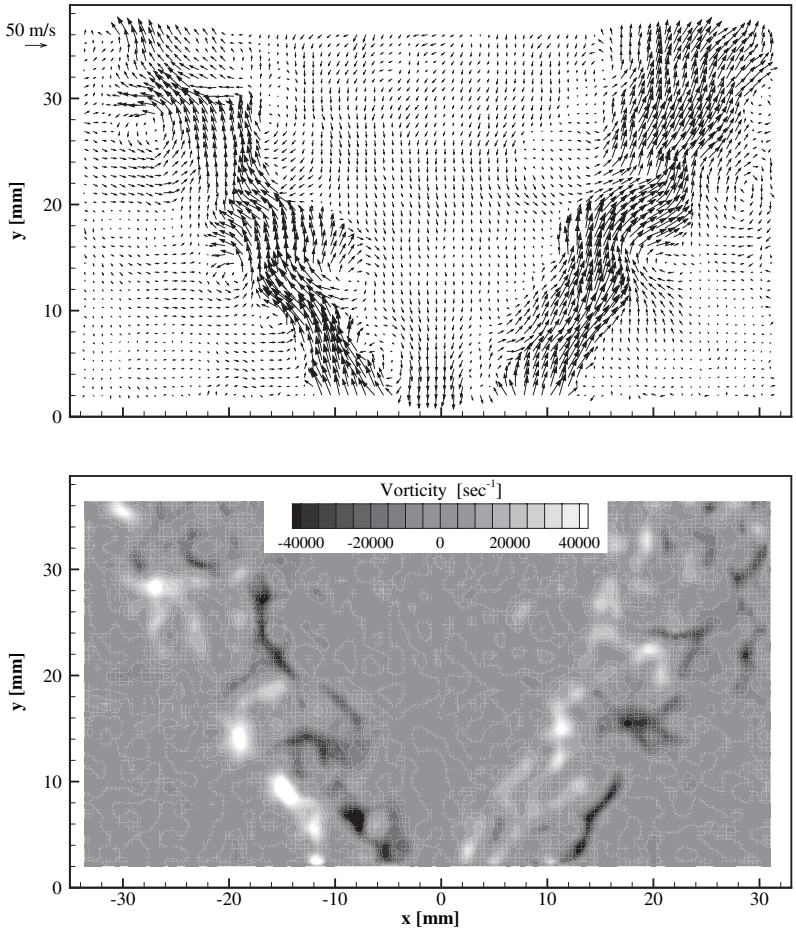

Fig. 9.76. Velocity map (top) and vorticity map (bottom) obtained at 3 bar.

The application of stereo PIV in facilities of this type is not trivial even if optical access seems sufficient. Aside from the loss of common viewing area caused by the oblique views of two cameras through a common window, further problems are introduced by the reflections of laser flare from the light sheet entering the test section through an orthogonal window. Hence the most desirable arrangement is the 'classical' normal view of the light sheet through a window that itself is parallel to it. For stereoscopic viewing the second camera will suffer from the reflection and occlusion effects described before such that reconstructed 3C velocity data will be available in a reduced area.

One solution to the limited access problem of multi-camera PIV imaging is to combine standard 2C PIV with Doppler global velocimetry (DGV) which

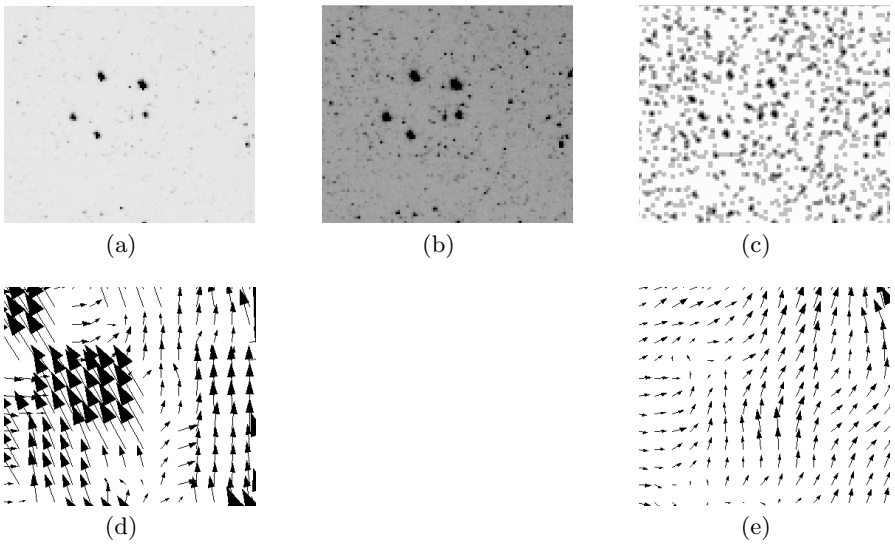

Fig. 9.77. Portion (120 × 100 pixel) of PIV recordings - inverted for clarity - and processed PIV data: a) fuel droplets, b) brightened version of a) with seeding visible, c) pre-processed image, d) flow field after standard PIV analysis, e) flow field obtained after enhancement of PIV images (from [377]).

has a sensitivity to the out-of-plane component [468, 471]. The so-called DGV-PIV method was applied to recover the velocity field inside the dilution zone of the single sector combustor [378]. Since the dilution zone could only be observed through two windows opposite to each other the light sheet was introduced through the top of the combustion chamber. Traversal of the entire acquisition system allowed the recovery of time-averaged volume resolved data sets of the dilution zone at pressures of up 10 bars [378].

In this particular application DGV and PIV were applied in succession due to technical limitations with the lasers used for illumination. Truly simultaneous DGV-PIV measurements could be demonstrated on a free jet experiment by Wernet [472].

9.15 A High-Speed PIV Study on Trailing-Edge Noise Sources

Contributed by:
A. Schröder, U. Dierksheide, M. Herr, T. Lauke

Table 9.20. PIV recording parameters for high-speed PIV (HS-PIV) measurements at the trailing-edge of a flat plate.

Flow geometry	perpendicular to trailing-edge
Maximum velocity	50 m/s
Field of view	$140 \times 37\,\mathrm{mm}^2$
Interrogation volume	$4 \times 4 \times 0.7\,\mathrm{mm}^3$
Dynamic velocity range	0 – 50 m/s
Observation distance	1.2 m
Recording method	double frame/single exposure/4 kHz
Recording medium	CMOS-camera
Recording lens	$f = 105\,\mathrm{mm}$, $f_\# = 1.8$
Illumination	Nd:YLF laser, 7 mJ per pulse
Pulse delay	$\Delta t = 20\,\mathrm{s}$
Seeding material	DEHS ($d_p \approx 1\,\mu\mathrm{m}$)

9.15.1 Introduction

Airframe noise is essentially due to the interaction of unsteady, mostly turbulent flow with the structure of the airplane, particularly caused by vortical flows around edges or over open cavities. A classical problem in this field is the trailing edge noise, which involves different noise generating mechanisms. Extensive investigations have been conducted on airfoil- and on flat plate trailing edges. According to [380, 381, 382] the major noise contribution is provided by the span-wise component of vorticity, the corresponding dipole ("principal edge noise dipole") is the sc. perturbed Lamb vector being perpendicular to the plane of the plate. A numerical simulation of trailing edge noise can be performed, based on such HS-PIV input data.

9.15.2 Setup, Measurements and Procedure

A flat plate (chord based $Re = 5.3 \times 10^6$ and 6.6×10^6) with profiled leading and trailing edges was mounted vertically in the Aeroacoustic Wind Tunnel Braunschweig (AWB), which is an open jet anechoic test facility (see Figures 9.78). The flat plate boundary layer was tripped at the leading edge, reaching a thickness of $\delta = 0.03\,\mathrm{m}$ on each side of the trailing edge, corresponding to free stream velocities of $U = 40\,\mathrm{m/s}$ to $50\,\mathrm{m/s}$ and a chord length of 2 m. Towards the trailing edge the plate is slightly and symmetrically convergent (5° taper), but no flow separation occurs. A full description of the experimental setup is provided in [379, 383]. The PIV measurement volume was located at the trailing edge in a x-y-plane within the turbulent boundary layer in order to track the flow structures with a spatial resolution of 256 pixel in y- and